THE JOURNAL OF BIOLOGICAL CHEMISTRY VOL. 290, NO. 10, pp. 6482–6494, March 6, 2015

A Parallel Quadruplex DNA Is Bound Tightly but Unfolded Slowly by Pif1 Helicase*

Received for publication, December 5, 2014, and in revised form, January 10, 2015 Published, JBC Papers in Press, January 14, 2015, DOI 10.1074/jbc.M114.630749

Alicia K. Byrd and Kevin D. Raney[1]

From the Department of Biochemistry and Molecular Biology, University of Arkansas for Medical Sciences, Little Rock, Arkansas 72205

Background: Some G-rich sequences fold into intramolecular quadruplex structures. Pif1 helicase reduces genomic instability by unfolding quadruplex DNA.
Results: Pif1 unfolds a parallel quadruplex structure slowly relative to unwinding of duplex DNA.
Conclusion: Comparison of duplex unwinding to quadruplex unfolding is complicated by distinct kinetic mechanisms.
Significance: A highly stable, intramolecular quadruplex is a formidable obstacle but can be overcome by Pif1 helicase.

DNA sequences that can form intramolecular quadruplex structures are found in promoters of proto-oncogenes. Many of these sequences readily fold into parallel quadruplexes. Here we characterize the ability of yeast Pif1 to bind and unfold a parallel quadruplex DNA substrate. We found that Pif1 binds more tightly to the parallel quadruplex DNA than single-stranded DNA or tailed duplexes. However, Pif1 unwinding of duplexes occurs at a much faster rate than unfolding of a parallel intramolecular quadruplex. Pif1 readily unfolds a parallel quadruplex DNA substrate in a multiturnover reaction and also generates some product under single cycle conditions. The rate of ATP hydrolysis by Pif1 is reduced when bound to a parallel quadruplex compared with single-stranded DNA. ATP hydrolysis occurs at a faster rate than quadruplex unfolding, indicating that some ATP hydrolysis events are non-productive during unfolding of intramolecular parallel quadruplex DNA. However, product eventually accumulates at a slow rate.

Helicases are ubiquitous enzymes that bind to and unwind double-stranded DNA (dsDNA) during DNA replication, repair, and recombination (for reviews, see Refs. 1–4). For many helicases, translocation along single-stranded DNA (ssDNA)[2] is related to their ability to melt dsDNA. Binding and hydrolysis of ATP are known to drive helicase movement along DNA. Hence, helicases are molecular motor proteins that have the ability to move along a ssDNA tracking strand, removing or displacing the complementary strand. However, the roles of helicases encompass more than simply separating dsDNA into ssDNA. Helicases also remove obstacles such as proteins and alternative secondary structures from DNA and remodel RNA. Proteins that act on DNA are likely to encounter a variety of secondary structures, including G-quadruplexes (G4) (5), triplexes (6), Z-DNA (7), and cruciforms (8), that can result in barriers to replication. A number of helicases have been observed to function on non-B-form DNA structures, in particular those of the RecQ and RecG families (for reviews, see Refs. 1 and 9). Sequences known to form alternative DNA structures are associated with genome instability and human disease (for a review, see Ref. 10).

G-quadruplexes are four-stranded structures stabilized by Hoogsteen base pairs between guanines in a planar ring that is referred to as a G quartet (for reviews, see Refs. 5 and 11). They can form from a single strand that has four tracts of three or more guanines separated by variable length loops characterized by the sequence motif $G_3N_{1-7}G_3N_{1-7}G_3N_{1-7}G_3$ (intramolecular G4) or from the association of multiple G-rich strands (intermolecular G4). Recently, several methodologies have provided convincing evidence that supports the formation of G4DNA in cells. Antibodies to G4DNA have been used to visualize G4DNA in both telomeric (12) and non-telomeric (13, 14) regions. Small molecules that are designed to interact specifically with G4DNA have been used to affinity purify quadruplexes from cells (15). *Saccharomyces cerevisiae* Pif1 helicase was shown to localize to G4DNA sequences (16) and to bind to and unfold G4DNA structures (17–19). The XPD and XPB helicases have also recently been found to co-localize with G4DNA in cells (20). Furthermore, introduction of G4DNA sequences elicits a replication block in the absence of appropriate translesion DNA polymerases (21). Currently, the structural mechanism for protein recognition of G4DNA and the specific function of G4DNA sequences remain to be determined, but several roles in DNA and RNA metabolism have been suggested (for reviews, see Refs. 5 and 11).

This putative quadruplex-forming motif is found throughout both the mitochondrial and nuclear genomes of many organisms, including yeast and humans (22–25), but is localized preferentially to certain regions such as promoters, often in proto-oncogenes (22, 26). The evolutionary conservation of these G4-forming sequences and clustering in certain regions of the genome suggests that these structures serve a purpose, although

* This work was supported, in whole or in part, by National Institutes of Health Grant R01 GM098922 (to K. D. R.). This work was also supported by the Arkansas Biosciences Institute, the major research component of the Arkansas Tobacco Settlement Proceeds Act of 2000.
[1] To whom correspondence should be addressed: Dept. of Biochemistry and Molecular Biology, Slot 516, University of Arkansas for Medical Sciences, 4301 W. Markham, Little Rock, AR 72205. Tel.: 501-686-5244; Fax: 501-686-8169; E-mail: raneykevind@uams.edu.
[2] The abbreviations used are: ssDNA, single-stranded DNA; G4, G-quadruplex; nt, nucleotides; K_d, equilibrium dissociation constant; FAM, fluorescein amidite; DMS, dimethyl sulfate; RHAU, RNA helicase associated with AU-rich element; Pif1h, Pif1 helicase domain.

they can also cause replication fork stalling and genomic instability (17, 18, 27–29). G4DNA can adopt many different forms, all of which have stacks of G-tetrads as the defining feature. However, G4DNA can vary in terms of the direction of each strand (parallel *versus* antiparallel), the number of different strands (intramolecular *versus* intermolecular), and the length of the DNA loops that occur between runs of guanines.

Several helicases have been shown to be able to unfold G4DNA. Pif1 helicase binds tightly to and readily unfolds a tetramolecular G4DNA quadruplex *in vitro* and reduces genomic instability (16, 18). Pif1 helicase (Pif1) has recently been reported to unfold an intramolecular G4; however, ssDNA product did not accumulate due to quadruplex refolding. The unfolding/refolding cycle occurred repetitively, leading the authors to conclude that Pif1 effectively "patrolled" the DNA (19). BLM and WRN helicases, both from the RecQ subfamily, have been found to unfold intramolecular G-quadruplexes (30). The FANCJ helicase unfolds both intermolecular and intramolecular G4DNA (31). RHAU is an RNA helicase that binds to and unfolds both tetramolecular (32) and intramolecular (33) G4DNA. A specific subdomain of RHAU has been proposed to interact with a guanine tetrad face of the quadruplex (34).

Most helicase unfolding experiments with G4DNA have been performed using tetramolecular quadruplex substrates such as that formed by the TPG4 sequence from the mouse immunoglobulin locus. Intramolecular quadruplexes have only been analyzed as substrates for a small number of helicases. Intramolecular quadruplexes have been proposed as the most likely *in vivo* target for many helicases. In the few cases that have been examined, some helicases can unfold intramolecular quadruplexes, but specific rates for unfolding have not been reported in most cases. It is important to determine the rates for unwinding of different DNA structures so that substrate preference can be defined.

Here we report the unfolding of an intramolecular parallel quadruplex and compare it with the rates for unfolding of a tetramolecular quadruplex and unwinding of a duplex by the *S. cerevisiae* Pif1. We chose the intramolecular quadruplex sequence from the promoter of the c-MYC proto-oncogene because of the wealth of literature describing its structure. A sequence involving the second through fifth guanines of the nuclease-hypersensitive element III_1 in the c-MYC promoter can be mutated at two sites (G14T and G23T) resulting in a highly stable structure of a single conformation that is the predominant conformation formed by the wild-type sequence in K^+ (35). Lack of knowledge about conformations or conformational heterogeneity of a substrate makes interpretation of results more complex because of the possibility of transitions between multiple conformations that, under some conditions, may be difficult to distinguish from unfolding of the G4DNA. The c-MYC sequence folds into a parallel quadruplex structure that has not been previously studied for Pif1 helicase and is the predominant type of G4DNA in the promoters of proto-oncogenes (36).

EXPERIMENTAL PROCEDURES

Materials—All oligonucleotides were purchased from Integrated DNA Technologies and purified as described (37). See Table 1 for sequences. Oligonucleotides were dissolved in 10 mM Tris-Cl, pH 7.5; quantified by UV absorbance using calculated extinction coefficients (38); and radiolabeled (39). Intramolecular quadruplexes were formed by incubation at 60 °C for 2 h in 10 mM Tris-Cl, pH 7.5, 100 mM KCl. Quadruplex formation was verified by circular dichroism (Fig. 1). Tetramolecular quadruplexes were formed as described (40). Pif1, K264A Pif1, Pif1 helicase domain (Pif1h) (41), and Dda (37) were purified as described.

dsDNA Unwinding and G4DNA Unfolding—All concentrations listed are final. 200 nM enzyme, unless otherwise specified, was preincubated with 2 nM radiolabeled DNA in Pif1 reaction buffer (25 mM Hepes, pH 7.5, 50 mM KCl, 2 mM β-mercaptoethanol, 0.1 mM EDTA, 0.1 mg/ml BSA). Reactions were initiated by addition of 5 mM ATP, 10 mM $MgCl_2$, and 60 nM (unless otherwise noted) DNA trap complimentary to the displaced strand (dsDNA) or G4-forming region (intramolecular G4). Reactions were quenched at various times with 400 mM EDTA, 0.1 mM T_{50} in nucleotides (nt) as a protein trap. Samples were separated by 15% (G4) or 20% (dsDNA) native PAGE, visualized using a Typhoon Trio phosphorimaging system, and quantitated using ImageQuant software (GE Healthcare). The fraction of substrate converted to product was determined and fit to a single exponential equation (G4 unfolding) or a four-step sequential mechanism (42, 43) (dsDNA unwinding) based on the known 1-bp step size of Pif1 (44) with 8 bp known to spontaneously melt at 25 °C (45).

DNA Binding—Substrate sequences are in Table 1. Fluorescein amidite (FAM)-labeled DNA (1 nM unless otherwise specified) was incubated with varying concentrations of enzyme in reaction buffer with 10 mM $MgCl_2$ for 30 min in the dark. Dda buffer contained 10 mM $Mg(OAc)_2$ and 10 mM KOAc instead of $MgCl_2$ and KCl. Polarization was measured in a PerkinElmer Life Sciences 1420 Victor^{3}V plate reader with excitation at 485 nm and emission at 535 nm. Data were fit to the quadratic equation to obtain a dissociation constant, K_d.

DNA Footprinting with Dimethyl Sulfate (DMS)—DMS footprinting reactions were performed in a fume hood. 20 nM c-MYC G4 substrate was incubated in the presence or absence of 500 nM Pif1 in 25 mM Tris, pH 7.5 with or without 100 mM KCl for 10 min at 25 °C. DMS was added to a final concentration of 5%. Reactions were quenched 5 s later by addition of 1.2 M β-mercaptoethanol, 15 mM EDTA, 1 μg/ml salmon sperm DNA, and 0.3 M NaOAc (final concentrations). After ethanol precipitation, samples were evaporated using a SpeedVac. The sample was resuspended in 90 μl 1 M piperidine, heated at 90 °C for 30 min, and evaporated to dryness. The residue was resuspended in 20 μl of H_2O and re-evaporated followed by resuspension in 10 μl of H_2O and re-evaporation to remove residual piperidine. Samples were resuspended in denaturing loading buffer (95% formamide, 0.025% sodium dodecyl sulfate, 0.025% bromphenol blue, 0.025% xylene cyanol), heated at 90 °C for 10 min, and separated on a denaturing 20% polyacrylamide gel. Samples were visualized using a Typhoon Trio phosphorimaging system and ImageQuant software. The radioactivity of each band of triplicate experiments was corrected for background. The average corrected radioactivity for each band was divided by the total radioactivity in the lane to determine the fraction. The relative reactivity associated with each base was deter-

TABLE 1

Sequences of oligonucleotides

Guanines involved in tetrad formation are underlined. Duplex-forming regions are colored.

Name	Use	Sequence
Duplex	Figs. 2, 7	5'-TTTTTTTTTTTTTTCGCTGATGTCGC-3' 5'-GCGACATCAGCGTTTTTTTTTTTTTT-3'
Duplex trap	Figs. 2, 7	5'-CGCTGATGTCGC-3'
Tetramolecular quadruplex	Fig. 2	5'-TGGACCAGACCTAGCAGCTATGGGGGAGCTGGGGAAGGT GGGAATGTGA-3'
c-MYC G4	Figs. 1, 4, 6, 10	5'-TTTTTTTTTTTTTTGAGGGTGGGTAGGGTGGGTAA-3'
Cy3 c-MYC G4	Figs. 1, 2, 6, 7, 8	5'-TTTTTTTTTTTTTTGAGGGTGGGTAGGGTGGGTAA-Cy3-3'
Trap	Figs. 2, 6, 7, 8	5'-CCCACCCTACCCACCC-3'
T15	Fig. 3	5'- TTTTTTTTTTTTTTT-6FAM-3'
5'-ss-quadruplex	Fig. 1, 3	5'-6FAM-TTTTTTTTTGGGTGGGTAGGGTGGGT-3'
5'-ss-duplex	Fig. 3	5'-6FAM-TTTTTTTTCGCTGATGTCGCCTGG-3' 5'-CCAGGCGACATCAGCG-3'
ssDNA	Fig. 3	5'- TTTTTTTT-6FAM-3'
Tailless quadruplex	Fig. 3	5'-TGGGTGGGTAGGGTGGGTTT-6FAM-3'
Cy3-Cy5 c-MYC G4	Fig. 1, 5	5'-Cy5-TTTTTTTTTTTTTTGAGGGTGGGTAGGGTGGGTAA-Cy3-3'
Forked G4DNA reporter	Fig. 9	5'-TTTTTTTTTTTTTTGAGGGTGGGTAGGGTGGGTAACGC TGATGTCGC-3' 5'-GCGACATCAGCGTTTTTTT-3'
No 5'-overhang forked reporter	Fig. 9	5'-TTTGAGGGTGGGTAGGGTGGGTAACGCTGATGTCGC-3' 5'-GCGACATCAGCGTTTTTTT-3'
Non-forked G4DNA reporter	Fig. 9	5'-TTTTTTTTTTTTTTGAGGGTGGGTAGGGTGGGTAACGC TGATGTCGC-3' 5'-GCGACATCAGCG-3'

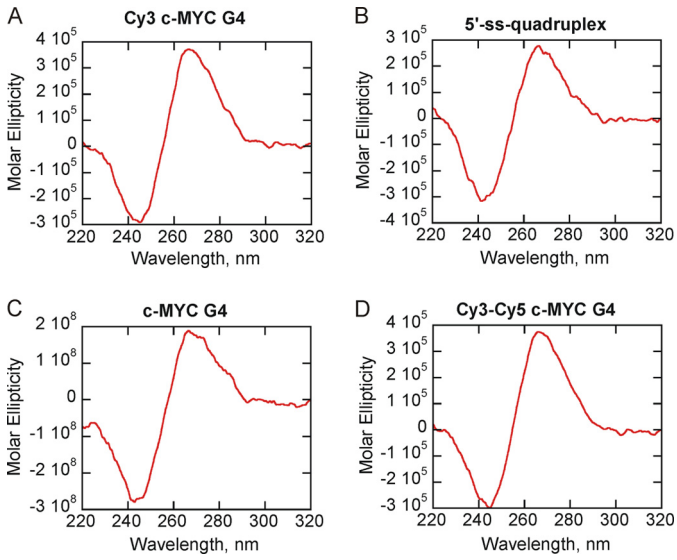

FIGURE 1. **CD spectra of oligonucleotides indicate formation of a parallel quadruplex.** CD spectra were obtained using a Jasco J-715 spectropolarimeter. Spectra of 10 μM DNA in 10 mM Tris, pH 7.5, 100 mM KCl exhibit a peak around 265 nm and a trough near 240 nm indicative of a parallel quadruplex. See Table 1 for DNA sequences.

mined by dividing the fraction in the presence of KCl by the fraction in the absence of KCl.

Measurement of G4 Folding by FRET—All concentrations are final. Cy3-Cy5-c-MYC G4 in reaction buffer without KCl with 10 mM $MgCl_2$ was mixed with 50 mM KCl in an SX.18MV stopped flow reaction analyzer (Applied Photophysics). The assay mixture was excited at 550 nm, and FRET was measured after a 665-nm cut-on filter (Newport Corp., catalog number 51330). Data were fit to a single exponential equation to obtain rate constants for folding.

Measurement of G4 Unfolding by FRET—All concentrations are final. Cy3-Cy5-c-MYC G4 (25 nM) was preincubated with 400 nM Pif1 in reaction buffer with 10 mM $MgCl_2$. Reactions were mixed with 5 mM ATP to initiate unfolding under instrumentation conditions as described for measurement of G4 folding.

ATPase Assay—Hydrolysis of ATP was measured using a spectrophotometric assay in which the hydrolysis of ATP is coupled by pyruvate kinase and lactate dehydrogenase to NADH oxidation. 50 nM Pif1 was added to reaction buffer with 10 mM $MgCl_2$, 5 mM ATP, 4 mM phosphoenolpyruvate, and 15 units/ml pyruvate kinase/lactate dehydrogenase. The change in

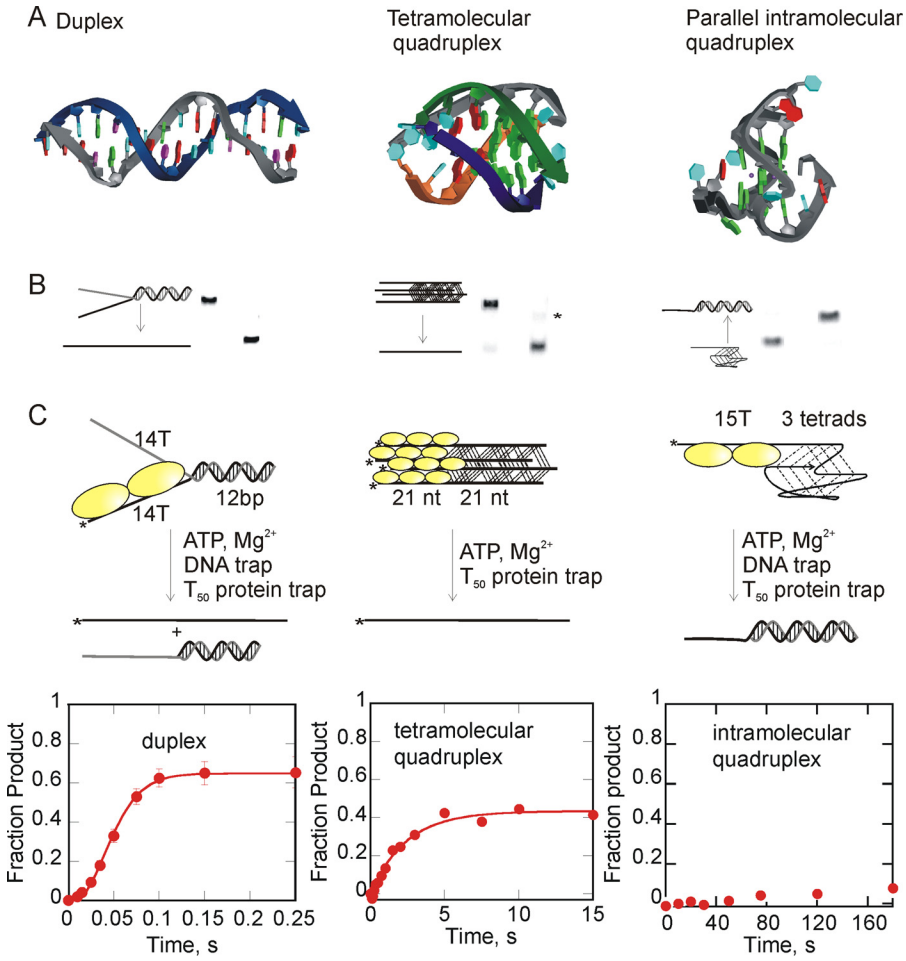

FIGURE 2. **Intramolecular parallel quadruplexes are a formidable obstacle to helicase progression.** *A*, structures of duplex DNA (Protein Data Bank code 3BSE (67)), tetramolecular quadruplex (Protein Data Bank code 1NP9 (68)), and intramolecular parallel quadruplex from the c-MYC promoter (Protein Data Bank code 1XAV (35)) illustrate the compact structure with sharp angles in the DNA backbone of an intramolecular quadruplex compared with the other DNA structures. *B*, duplex and tetramolecular G4 substrates can be separated from ssDNA products by native PAGE. A small amount of intermediate (*) is visible during unwinding of the tetramolecular substrate. A trapping strand must be added to intramolecular G4 to prevent refolding of the intramolecular quadruplex after melting and to allow the substrate and product to be separated by PAGE. *C*, substrate (2 nM for duplex and intramolecular G4 and 50 pM for tetramolecular G4) was preincubated with 200 nM Pif1, and a protein trap was added when the reaction was initiated to ensure single cycle conditions. The forked duplex was unwound at 76 ± 3 bp/s based on a fit to a four-step sequential mechanism. The tetramolecular G4 was unwound at 0.48 ± 0.11 s^{-1} based on a single exponential fit of the data. The amplitude of the product formation curve for the intramolecular G4 was not sufficient in a single cycle for fitting the data. Duplex and intramolecular G4 results are the average and S.D. of three independent experiments. Duplicate experiments of tetramolecular G4 unwinding produced similar results. *Error bars* represent S.D.

absorbance at 380 nm was monitored upon addition of 3 μM T_{15} or T_{15}-cMYC or 45 μM nt poly(dT) so that the concentration of ssDNA in nucleotides was constant in each case. The rate of NADH oxidation correlates directly with ATP hydrolysis.

RESULTS

Pif1 Unfolds Very Little Parallel Quadruplex in a Single Binding Event—The DNA backbone in duplex DNA and tetramolecular G4DNA is in a helical conformation that presents a similar track for sequential helicase movement (Fig. 2*A*). However, a parallel quadruplex folds into a compact, highly stable structure that may interact with the helicase differently (Fig. 2*A*). Both a duplex and a tetramolecular quadruplex migrate slowly on a native polyacrylamide gel relative to the migration of ssDNA (Fig. 2*B*). In contrast, intramolecular quadruplexes migrate at a similar rate through a native gel when compared with the ssDNA form, making it difficult to separate intramolecular quadruplexes from their ssDNA counterparts. Furthermore, intramolecular quadruplexes can refold after unfolding by helicases; thus a trapping strand is required to prevent spontaneous refolding. The trapped product migrates more slowly than the corresponding G4DNA allowing for separation by PAGE (Fig. 2*B*).

Unwinding or unfolding of various DNA structures under single cycle conditions with respect to substrate was compared because these conditions eliminate the effect of association on the observed kinetics. It should be noted that single turnover conditions refer to the action of all Pif1 molecules initially bound to the DNA substrate before dissociation of those enzyme molecules. There are likely multiple Pif1 molecules bound to each substrate molecule under these conditions. Pif1 has been reported to preferentially unwind forked duplexes (44, 46), tetramolecular quadruplexes (17, 18), and hybrid quadruplexes (19). In a single binding event, Pif1 rapidly unwinds a forked dsDNA at 76 ± 3 bp/s, whereas the tetraplex substrate is unwound at 0.48 ± 0.11 s^{-1} (Fig. 2*C*). The rate for unwinding of the duplex was derived from fitting the data to a four-step,

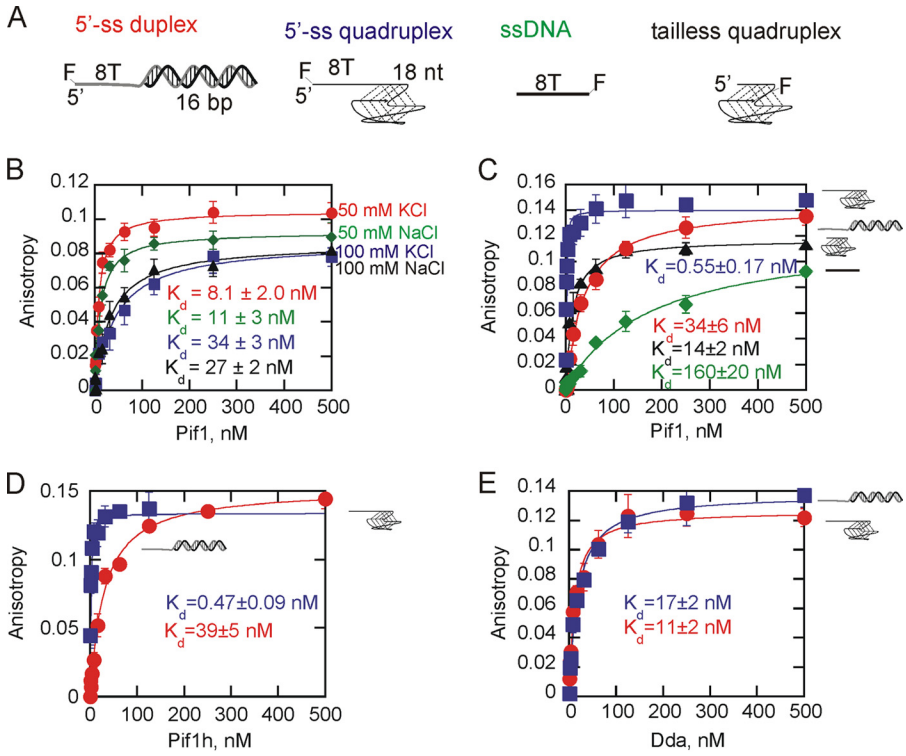

FIGURE 3. **Pif1 binds preferentially to a quadruplex-containing substrate.** *A*, diagrams illustrating the 5′-tailed duplex, 5′-tailed quadruplex, single-stranded DNA, and tailless quadruplex binding substrates are shown. *B*, fluorescence anisotropy of 1 nM T_{15} with increasing concentrations of Pif1 was measured at varying salt concentrations. Data were fit to the quadratic equation to obtain dissociation constants (K_d). Fluorescence anisotropy of samples containing 1 nM tailed duplex DNA (*red circles*) or 0.2 nM tailed G4DNA (*blue squares*) with increasing concentrations of Pif1 (*C*), Pif1h (*D*), and Dda (*E*) was measured. Anisotropy of 1 nM ssDNA (*green diamonds*) and 1 nM tailless G4DNA (*black triangles*) was also measured for Pif1. The affinity of Dda helicase was measured with a 1 nM concentration of each substrate. *Error bars* represent S.D.

stepwise mechanism that accounts for the lag phase in the progress curve. The rate for tetraplex unwinding is the result of a single exponential fit of the data. It is not known whether the tetraplex is unwound in a stepwise fashion similar to duplex DNA; hence the reported rate is for appearance of the single-stranded product. Interestingly, the tetraplex did not exhibit a lag phase, suggesting that the unwinding mechanism for this substrate contains mechanistic steps that are not present during duplex unwinding because a uniform stepping mechanism should result in a lag phase (42). Pif1 unfolds very little parallel intramolecular quadruplex (Cy3-c-MYC G4) under single cycle conditions (Fig. 2*C*). Increasing the Pif1 concentration did not increase the rate or amplitude for unwinding of any of the three substrates in Fig. 2 (not shown).

Pif1 Binds Tightly to a Parallel, Intramolecular Quadruplex through Its Helicase Domain—Pif1 appeared less able to unfold the intramolecular parallel G4DNA but has been reported to preferentially bind to and unfold tetramolecular G4 (18). Additionally, Pif1 maps to regions in chromosomes likely to form intramolecular G4DNA (16), so we sought to determine the affinity of Pif1 for intramolecular G4DNA relative to ssDNA and dsDNA substrates. Fluorescently labeled DNA substrates were incubated with increasing concentrations of Pif1, and anisotropy was measured. Previously, *in vitro* Pif1 reactions have been reported in 50 or 100 mM NaCl (44, 47, 48). Because quadruplex stabilities and structures can vary in Na^+ *versus* K^+ (49–51), the affinity of Pif1 for ssDNA was compared in buffers containing both 50 and 100 mM concentrations of each cation (Fig. 3*B*). Binding was tighter at lower salt concentrations, but no difference was observed in Na^+ *versus* K^+, indicating that buffers containing K^+ are suitable for *in vitro* Pif1 reactions.

The affinity of Pif1 for duplex DNA *versus* intramolecular G4DNA, both with a 5′-T_8 ssDNA tail, was directly compared with ssDNA and a substrate containing only G4DNA (tailless G4) (Fig. 3*C*). Pif1 was found to bind to the tailed G4DNA substrate with a K_d value of 0.55 ± 0.17 nM, which is a 60-fold greater affinity than binding to the tailed dsDNA. Pif1 also binds to a substrate containing only G4DNA, although the affinity is reduced (14 ± 2 nM). A truncated variant of Pif1 was prepared in which portions of the N terminus and C terminus were removed. This variant, referred to as Pif1h, bound to the G4 substrate with a similar affinity as full-length Pif1 (Fig. 3*D*). Additionally, this high affinity for G4DNA is not a general feature of superfamily 1B helicases because Dda, a member of the same helicase family as Pif1, does not exhibit increased affinity for G4-containing substrates (Fig. 3*E*).

Binding of Pif1 to the G4DNA does not affect the G4 structure as determined by DMS footprinting (Fig. 4). DMS reacts with the N7 atom of guanine, which is protected in G4DNA but is accessible in ssDNA and dsDNA. The DMS footprinting pattern exhibits protection at guanines that form each tetrad in the presence of KCl (Fig. 4*A*). The protection pattern does not change at these guanines in the presence of Pif1 (Fig. 4, *A* and *B*), indicating that Pif1 binding does not disrupt the G4 structure.

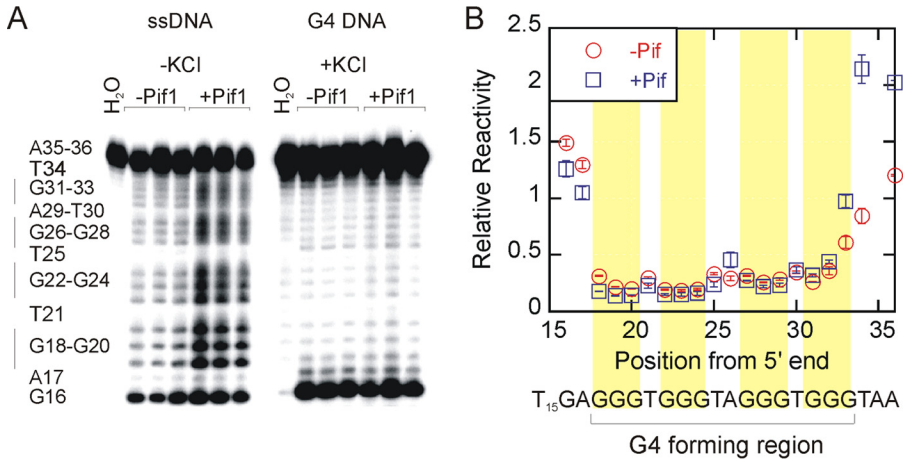

FIGURE 4. **Pif1 binding does not affect the intramolecular quadruplex structure.** *A*, the c-MYC G4DNA was subjected to DMS footprinting in the absence and presence of Pif1 on both ssDNA (−*KCl*) and G4DNA (+*KCl*) to examine the effect of Pif1 on the G4 structure. *B*, the relative reactivity of the bases was compared in the presence and absence of KCl. The low reactivity of each guanine in the G4-forming region (*yellow*) indicates protection due to Hoogsteen base pairing in G4DNA in the presence of KCl (*open red circles*). Guanines involved in tetrad formation remain protected upon addition of Pif1 (*open blue squares*). *Error bars* represent S.D.

The c-MYC G4DNA Sequence Folds Slowly into a Quadruplex Structure—Pif1 binds tightly to intramolecular G4 but does not produce significant quantities of product in a single cycle unfolding reaction, raising the question of whether Pif1 unfolds the quadruplex but the DNA refolds before it can be trapped. This possibility would require a very rapid folding rate to prevent the unfolded G4 sequence from hybridizing to the trapping strand (Fig. 2*C*). To measure folding, the c-MYC G4DNA sequence was prepared with Cy3 and Cy5 labels on the 3′-end and 5′-end, respectively. When the substrate is folded, the FRET pairs are in close proximity, resulting in a high fluorescence signal that is lost when the G4DNA is unfolded (Fig. 5*A*). Upon rapid mixing with KCl, the c-MYC G4 sequence folds with a rate constant of 0.05 s^{-1} (Fig. 5*B*), which is slightly faster but similar to that reported previously for this sequence (52, 53). The relatively slow folding rate indicates that rapid, Pif1-catalyzed unfolding followed by rapid folding of the parallel quadruplex does not occur. Other intramolecular G4 sequences have been reported to fold at widely varying rates. The human telomeric sequence has been reported to fold on time scales ranging from a few milliseconds to an hour (54, 55) possibly due to its conformational heterogeneity. When Pif1 is preincubated with folded G4, it can unfold the G4 in an ATP-dependent manner to produce ssDNA (Fig. 5*C*).

Pif1 Unfolds Parallel G4DNA under Multiple Turnover Conditions—We investigated the ability of Pif1 to unfold the c-MYC G4DNA in a multiturnover reaction in the presence of the complementary trapping strand (Fig. 6). Pif1 (200 nM) readily unfolded the parallel c-MYC G4DNA (2 nM) in the presence of 60 nM trapping strand (Fig. 6*B*). Raising the concentration of Pif1 did not increase the observed rate of product formation. The reaction was dependent on the presence of ATP, indicating that the trapping strand does not spontaneously hybridize to the G4DNA under these conditions. The trapping strand concentration could be reduced with only modest effects on the rate and amplitude for unfolding (Fig. 6*C*). Remarkably, even 15 nM trapping strand could hybridize with most of the ssDNA product, suggesting that Pif1 may assist in annealing the complementary strand. Pif1 has been reported to facilitate annealing of complementary strands under conditions of low DNA concentrations (56). The results were similar when the reaction was initiated with addition of ATP-bound Pif1 (Fig. 6*D*), indicating that the order of addition does not affect the results. Although Pif1 does unfold the intramolecular c-MYC G4DNA in a multiturnover reaction, the rate is more than 100-fold slower than the rate of dsDNA unwinding. However, product does accumulate, and the majority of the G4DNA substrate is eventually converted to product.

Although no product formation was observed in the absence of ATP (Figs. 5*C* and 6*B*) and Pif1 binding had no effect on the G4DNA structure (Fig. 4*B*), it is possible that ATP-bound Pif1 could result in product formation. To test this possibility, G4DNA unfolding (Fig. 7*A*) and dsDNA unwinding (Fig. 7*B*) reactions were performed with an ATPase-dead Pif1 variant. This form of the enzyme has an alanine replacing the catalytic lysine (K264A) in the Walker A motif (17). Product formation was negligible in each case, indicating that ATP hydrolysis by Pif1 is necessary for G4DNA unfolding and dsDNA unwinding.

To determine whether the observed rate was limited by Pif1-catalyzed unfolding of the G4DNA, similar experiments were performed at much higher concentrations of G4DNA, Pif1, and trapping strand. Increasing the concentrations of enzyme and substrate should increase association events, whereas increasing the trapping strand should speed up hybridization with unfolded c-MYC G4DNA substrate. When the DNA trapping strand was raised to 1 μM, the G4DNA was observed to hybridize with the trapping strand in the absence of Pif1 (not shown) as reported to occur previously at high concentrations of DNA complementary to G4DNA (57). However, enzyme-catalyzed unfolding of the c-MYC G4DNA was much faster than unfolding due to the trap alone. Therefore, a protocol was developed in which a second trapping strand could be introduced to hybridize to the first trapping strand upon quenching of the reaction so that only Pif1-catalyzed unfolding could be observed. G4DNA (200 nM) was incubated with Pif1 (3 μM) followed by initiation of the unfolding reaction by addition of

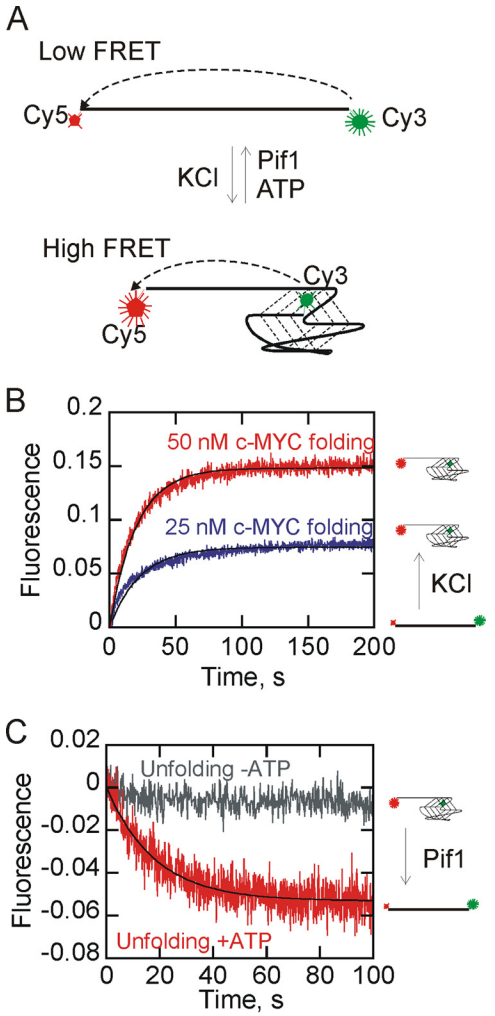

FIGURE 5. **Folding and unfolding of the c-MYC intramolecular quadruplex.** *A*, folding and unfolding of a Cy3-Cy5-labeled c-MYC G4 substrate can be monitored by changes in FRET. *B*, folding of 25 nM c-MYC DNA (*blue*) and 50 nM DNA (*red*) upon addition of KCl was fit to a single exponential equation. The rate constants were 0.051 ± 0.001 s^{-1} for 25 nM DNA and 0.049 ± 0.002 s^{-1} for 50 nM DNA. *C*, unfolding of 25 nM Cy3-Cy5-c-MYC G4 by 400 nM Pif1 was measured, and data were fit to a single exponential equation to obtain the observed rate constant (0.048 ± 0.011 s^{-1}). Unfolding was not observed in the absence of ATP (*gray*).

ATP, $MgCl_2$, and the quadruplex trapping strand (1 μM; termed *Qtrap* in Fig. 8*A*). At increasing times, the quench solution was added to stop Pif1-catalyzed unfolding of c-MYC G4DNA. Along with the quencher, a second trapping strand, which was simply the unlabeled c-MYC G4DNA sequence (termed *Ctrap* in Fig. 8*A*), was added. The unlabeled c-MYC G4DNA sequence hybridized to any quadruplex trapping strand that was not hybridized to unfolded G4DNA. This allowed Pif1-catalyzed unfolding to occur but prevented "trap-catalyzed" unfolding because the trap simply hybridized to the excess unlabeled c-MYC G4DNA. These conditions allowed measurement of the rate of G4DNA unfolding with 3 μM Pif1 and 1 μM trapping strand. Little product was observed under single cycle reaction conditions, again indicating that the c-MYC G4DNA is unfolded slowly in a single binding event. Under multiturnover conditions (Fig. 8*C*), Pif1 unfolded the parallel G4DNA at a rate similar to that observed at lower enzyme and substrate concentrations, indicating that the observed rates are indeed limited by Pif1-catalyzed unfolding of G4DNA.

Pif1 Unwinds a Duplex Past a Quadruplex—To further explore unfolding of the parallel G4DNA, a substrate was designed with a reporter duplex adjacent to the G4DNA (Fig. 9*A*). The reporter duplex was designed to contain a 3′-tail so that after unfolding of the G4DNA Pif1 would encounter a short forked duplex substrate, which is readily unwound (Fig. 2*C*). A control substrate (Fig. 9*B*) lacked a 5′-tail to ensure that no dsDNA unwinding would occur in the absence of G4DNA unfolding. Labeling the displaced strand of the reporter duplex provided a clear report on the ability of Pif1 to unfold the G4DNA (Fig. 9*C*). The G4DNA substrate was unfolded in both multiturnover and single cycle conditions (Fig. 9*C*), although only 15% of the reporter duplex was unwound in a single cycle (Fig. 9*D*). Product formation was nearly non-existent over the time frame of the reaction when the G4DNA substrate lacked a 5′-overhang (Fig. 9*D*), indicating that formation of product was due to unfolding of the G4DNA followed by dsDNA unwinding.

Pif1 has previously been reported to be unable to unwind a 21-base pair duplex past a quadruplex (19). However, Pif1 preferentially unwinds short forked duplex substrates (44, 46), and the duplex reporter in the previous report was not forked, which would have decreased the ability of Pif1 to unwind it. The reporter duplex in these experiments is a 12-base pair forked duplex; thus it is efficiently unwound by Pif1 (Fig. 2*C*).

Because unwinding of the reporter duplex is much more rapid (Fig. 2*C*) than the result with the parallel G4DNA, the observed rate is limited by the rate of Pif1-catalyzed G4DNA unfolding. The rate of G4DNA unfolding determined by the reporter assay, 0.11 ± 0.01 s^{-1}, is similar to that measured in previous assays that relied on trapping the unfolded quadruplex (0.063 ± 0.013 s^{-1} in Fig. 6 and 0.066 ± 0.010 s^{-1} in Fig. 8).

A similar substrate was designed that lacked an overhang on the displaced strand so that the duplex would not be forked (Fig. 9*E*). Under multiturnover conditions (Fig. 9, *F* and *G*), unwinding was similar to that of the forked duplex (Fig. 9, *C* and *D*). However, no unwinding was observed under single cycle conditions (Fig. 9*G*, *green*). Thus, even a 12-base pair non-forked duplex located downstream of a parallel quadruplex cannot be unwound by Pif1 in a single cycle.

ATP Hydrolysis Slows at G4DNA—Helicases utilize the energy of ATP hydrolysis to unwind DNA. The rate of ATP hydrolysis by Pif1 on a long ssDNA, ssDNA of the same length as the ssDNA binding site on the G4DNA substrate, and G4DNA with a 5′-ssDNA tail was compared. ATP hydrolysis rates were reduced 2.5-fold on G4DNA relative to ssDNA (Fig. 10). On both ssDNA and G4DNA, addition of a greater concentration of DNA failed to increase the ATPase rate (not shown), indicating that these are the maximal rates of ATP hydrolysis on these substrates. Although the ATPase rate is reduced on G4DNA, the measured rate, 31 s^{-1}, is still significantly faster than the G4 unfolding rate, 0.11 s^{-1}, indicating that many ATP hydrolysis events on c-MYC G4DNA are non-productive. This suggests that a parallel, intramolecular quadruplex is a formidable obstacle to Pif1 helicase progression. The rates of ATP hydrolysis and translocation on ssDNA are essentially equivalent for Pif1 (44). However, for this G4 substrate, not only is the

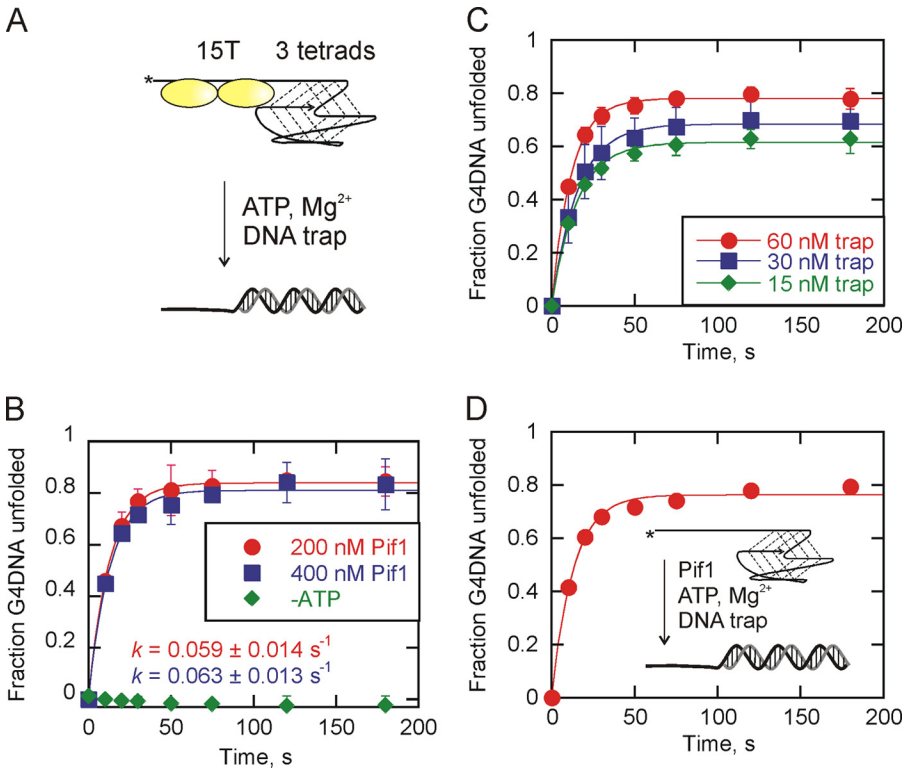

FIGURE 6. **Pif1 slowly unfolds an intramolecular quadruplex in the absence of a protein trap.** *A*, products of unfolding of a parallel G4DNA are trapped as dsDNA by a complementary strand. * indicates radiolabel. *B*, unfolding of 2 nM DNA by 200 nM and 400 nM Pif1 indicates that 200 nM is a saturating concentration. Data were fit to a single exponential equation to obtain rate constants of 0.059 ± 0.014 s^{-1} with 200 nM Pif1 and 0.063 ± 0.013 s^{-1} with 400 nM Pif1. Product formation was negligible in the absence of ATP. *C*, unfolding of 2 nM G4DNA by 400 nM Pif1 indicates that product is trapped even at 15 nM trapping strand, although the amplitude of the product formation curve is slightly reduced as the trap concentration decreases from 60 to 15 nM. Data were fit to a single exponential equation to obtain rate constants of 0.071 ± 0.012 s^{-1} with 60 nM trap, 0.064 ± 0.019 s^{-1} with 30 nM trap, and 0.066 ± 0.017 s^{-1} with 15 nM trap. *D*, unfolding of 2 nM DNA by 400 nM Pif1 was initiated by addition of Pif1, ATP, and Mg^{2+} to G4DNA. Data were fit to a single exponential equation to obtain a rate constant of 0.078 s^{-1}. *Error bars* represent S.D.

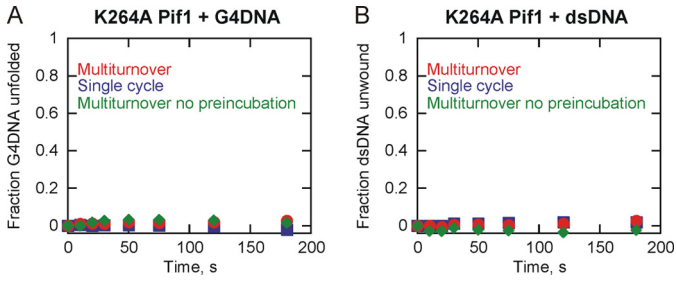

FIGURE 7. **An ATPase-dead Pif1 does not unfold an intramolecular quadruplex or duplex DNA.** K264A Pif1 was preincubated with parallel G4DNA (*A*) or duplex DNA (*B*), and the reaction was initiated by addition of ATP and Mg^{2+} to investigate product formation in the absence of ATP hydrolysis under multiturnover conditions (*red circles*) and under single cycle conditions (*blue squares*). Multiturnover reactions were also initiated by addition of K264A Pif1, ATP, and Mg^{2+} to the parallel G4DNA. In each case, product formation was negligible over the time frame tested.

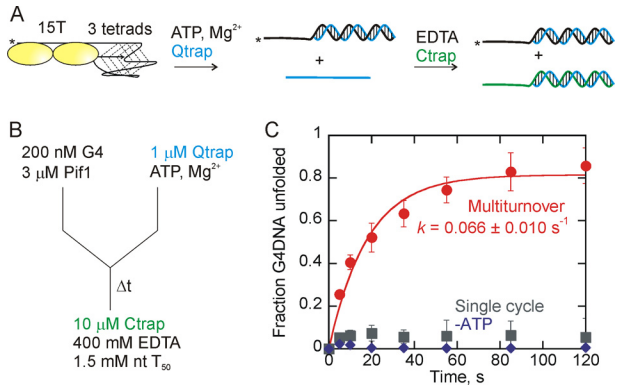

FIGURE 8. **The rate of unfolding of the parallel intramolecular G4DNA does not increase when trapping strand concentration is raised to 1 μM.** *A*, products of unfolding of a parallel intramolecular G4DNA are trapped as dsDNA by 1 μM quadruplex trap (*Qtrap*; *blue*). To prevent spontaneous unfolding of the G4DNA by the quadruplex trap, excess unlabeled, unfolded G4 DNA (*Ctrap*; *green*) is added to the reaction mixture along with the quench solution to sequester excess quadruplex trap. A schematic of the reaction setup is shown in *B* for clarity. *C*, data were fit to a single exponential equation to obtain a rate constant of 0.066 ± 0.010 s^{-1} for unfolding under multiturnover conditions (*red circles*). When a protein trap (1.5 mM T_{50} in nucleotides) was included (single cycle conditions; *gray squares*), insufficient product was formed to produce a reliable fit of the data. Under multiturnover conditions in the absence of ATP (*blue diamonds*), product formation was negligible during the time frame of the reaction. *Error bars* represent S.D.

ATPase rate reduced, but the rate of unfolding is further reduced.

DISCUSSION

Substrate preference for an enzyme is typically evaluated through kinetic analysis. Steady state kinetics can yield the second order rate constant k_{cat}/K_m, which is the standard measure for comparison of two substrates. The unique nature of a DNA polymer as an enzyme substrate presents problems that are not readily overcome when evaluating the preference for different substrates. For this reason, helicase-catalyzed DNA unwinding is not usually evaluated in terms of steady state kinetics because the substrate is not converted to a chemically distinct product but instead undergoes a local conformational change. Helicase

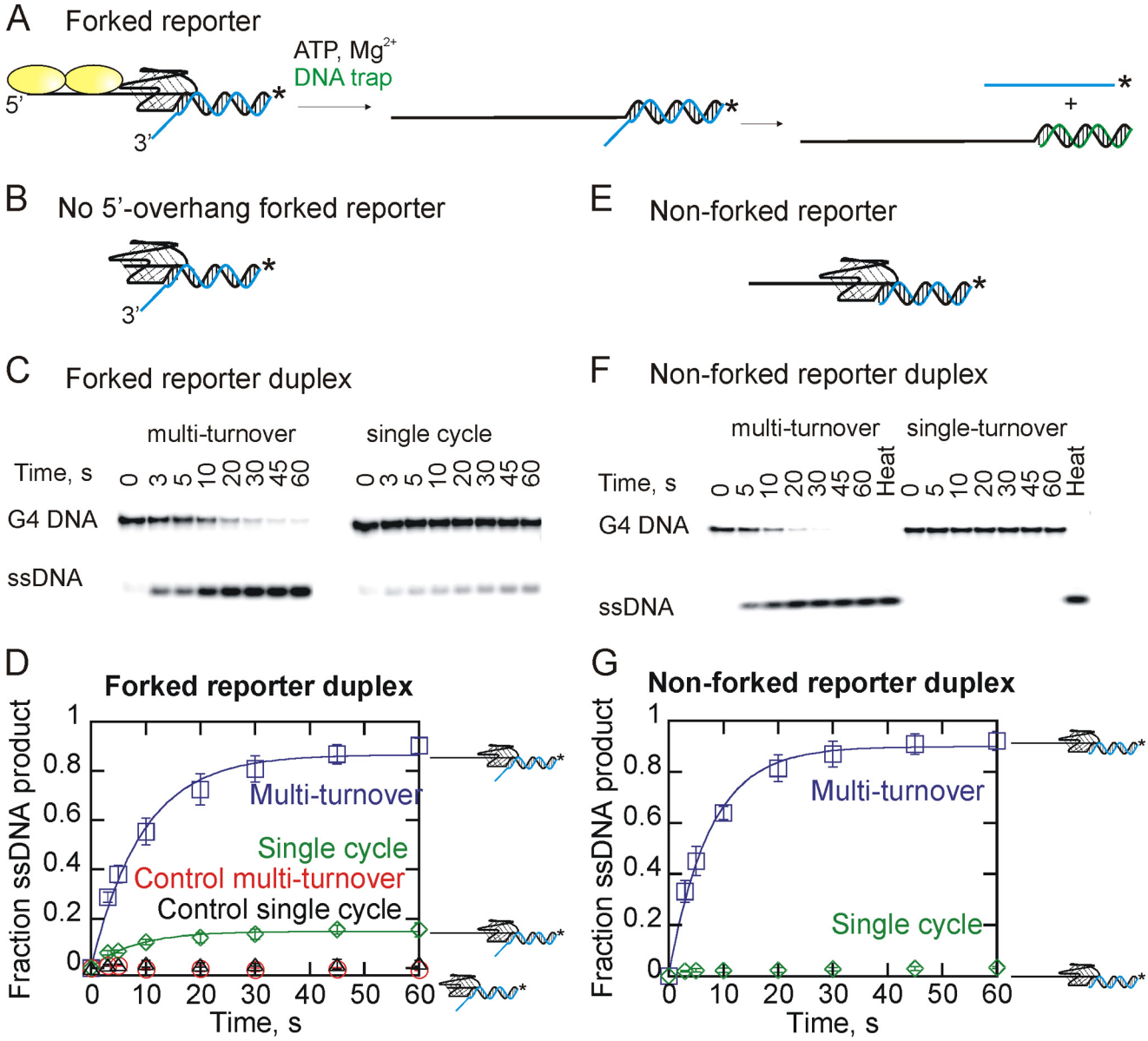

FIGURE 9. **Pif1 unwinds a reporter duplex after unfolding an intramolecular G4DNA.** *A*, schematic diagram illustrating the reaction. If Pif1 unfolds the intramolecular G4DNA, helicase activity can proceed to rapidly unwind the forked duplex containing the radiolabeled strand (*blue*). * indicates radiolabel. *B*, control reactions were performed with a G4DNA forked reporter duplex lacking a 5′-overhang to ensure that unfolding of the G4DNA occurred prior to displacement of the labeled strand (*blue*). *C*, products of G4DNA unfolding/forked duplex unwinding were separated by 20% PAGE. *D*, in both multiturnover (*open squares*) and single cycle reactions (*open diamonds*), the G4DNA substrate was unfolded as measured by unwinding of the reporter duplex. The control substrate lacking the 5′-overhang was not unwound under multiturnover (*open circles*) or single cycle (*open triangles*) conditions. Data were fit to a single exponential equation to obtain a rate constant of 0.11 ± 0.01 s^{-1} for unfolding of the intramolecular G4DNA in a multiturnover reaction. Under single cycle conditions, the amplitude of G4DNA unfolding was 0.15 ± 0.01 based on a single exponential fit of the data. The rate constant was 0.085 ± 0.001 s^{-1}. *E*, diagram illustrating the non-forked reporter duplex colored as in *A*. *F*, products of G4DNA unfolding/non-forked duplex unwinding were separated by 20% PAGE. *G*, in a multiturnover (*open squares*) reaction, the G4DNA substrate was unfolded as measured by unwinding of the reporter duplex (rate constant of 0.13 ± 0.02 s^{-1}); however, unwinding under single cycle conditions (*open diamonds*) was not observed. *Error bars* represent S.D.

activity is defined in terms of equilibrium binding constants, rates for unwinding, processivity for unwinding, and step size. Many of these parameters can be obtained during single cycle kinetic analysis in which the helicase activity is evaluated in a single binding event. In this report, we provide an initial kinetic analysis for single cycle, helicase-catalyzed unfolding of an intramolecular, parallel quadruplex DNA substrate. *S. cerevisiae* Pif1 helicase has been well characterized through pioneering work from Zakian and co-workers (16, 18). This group already has identified Pif1 as capable of unfolding quadruplex DNA (16, 18). For the current study, we chose a G-rich DNA sequence that was well characterized and folds into a conformation that has yet to be examined for unfolding by Pif1. The c-MYC promoter sequence is known to adopt primarily one conformation, the intramolecular parallel quadruplex. The promoters of human proto-oncogenes frequently contain sequences that fold into G4DNA (22) with the parallel structure being the most common (36). Pif1-catalyzed unfolding rates of tetramolecular and intramolecular parallel G4DNA are slower than unwinding of duplex DNA based on the substrates used

here (Fig. 2). However, the rate and extent of unwinding *in vitro* does not address the tight binding observed for tetramolecular quadruplexes (18) and intramolecular parallel quadruplexes (Fig. 3).

Several reports indicate that G4DNA substrates are unwound better than duplex substrates for some helicases, including Pif1 (17, 20, 31). The comparison of substrates can be complicated by the significant differences in structure and in the number of potential binding sites that can support helicase activity. The G4DNA substrate in a tetramolecular species contains four ssDNA overhangs adjacent to the G-tetrad. Therefore, four potential entry sites are available for a helicase to bind and translocate into the quadruplex. For comparison, a duplex substrate will have only one strand on which the helicase can bind to and translocate along except for a few exceptions such as the RecBCD helicase (58). The difference in the number of ssDNA tracks on which a helicase can bind to melt a quadruplex is perhaps the most difficult issue to control.

The mechanism for duplex unwinding exhibited by many helicases, including Pif1, is a stepwise, 1 base pair per step movement coupled to the hydrolysis of one molecule of ATP (44, 59). The mechanism for other helicases has been suggested to involve buildup of strain so that multiple ATP hydrolysis events can occur followed by unzipping of 2 or more base pairs per step (60). In either case, the helicase does not melt more than a few base pairs per step. These stepwise mechanisms allow the helicase to unwind very stable duplex structures for tens to thousands of base pairs.

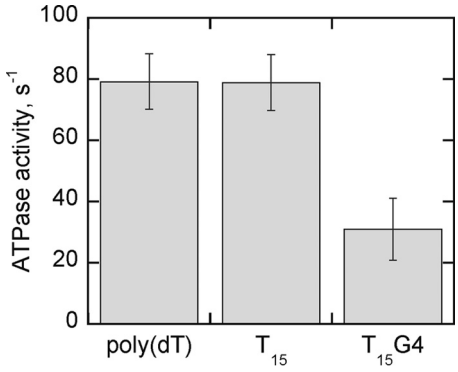

FIGURE 10. **ATP hydrolysis by Pif1 slows on parallel G4DNA.** The rate of ATP hydrolysis by Pif1 was measured on poly(dT) ($80 \pm 9\ s^{-1}$), T_{15} ($79 \pm 9\ s^{-1}$), and T_{15}G4 (c-MYC G4) ($31 \pm 10\ s^{-1}$), each at a concentration of 3 μM 15-mer. The rates are shown with S.D. of three independent experiments. *Error bars* represent S.D.

In the case of duplex DNA, around 8–10 base pairs melt spontaneously at 25 °C (45), meaning that a helicase need not actively melt the final few base pairs for ssDNA product to form. The number of bases that need to be disrupted to unfold a quadruplex is less well characterized and may vary depending on the type and stability of the quadruplex but must be considered to compare helicase activity on different types of DNA substrates. Some evidence from single molecule experiments indicates that only a few bases need to be disrupted from an intramolecular quadruplex to cause the remaining structure to unfold (61). Additionally, the binding action of a translesion polymerase at a quadruplex template disrupted the structure of the quadruplex (53). This suggests that in the case of the intramolecular quadruplex stepwise mechanisms similar to those involved in dsDNA unwinding may not apply because the inherent stability of the structure may change dramatically with the removal of a few bases, and disruption of the remaining structure may occur. If all the guanines within the first three columns of the c-MYC G4DNA must be traversed by the helicase, then multiple steps might be required for complete unfolding. However, if only a few nucleotides must be removed to result in complete unfolding of the quadruplex, then only a few steps would be required. In either case, these steps must be much slower for the c-MYC quadruplex than steps observed for duplex DNA unwinding. The stability of the tetramolecular quadruplex is reportedly greater than that of the intramolecular parallel quadruplex (Table 2) (62). The fact that the tetramolecular quadruplex is melted faster and to a greater extent by Pif1 than the intramolecular parallel quadruplex indicates that unfolding is not strictly related to the inherent stability of the substrate. It is possible that the stepwise movement of a helicase coupled with the ability of multiple helicase molecules to act on the substrate simultaneously may allow the helicase to readily "peel" off one of the strands of the tetraplex. For the intramolecular quadruplex, the arrangement of the DNA backbone may preclude the straightforward, stepwise unzipping mechanism. The thermal stability of duplex DNA is significantly lower than that of G4DNA of a comparable length. It is possible that the

TABLE 2
Binding affinities and unwinding rates for different substrate types

Substrate	K_d	Unwinding rate	Fraction unwound	Melting temperature
	nM			*°C*
Duplex	34 ± 6[a]	76 ± 3 bp/s[b]	0.65 ± 0.10[k]	40[c]
Duplex (20 bp)	34 ± 6[a]	75 ± 12 bp/s[d]	0.26 ± 0.10[d]	65[c]
Tetramolecular G4	0.08[e]	10 ± 2 nt/s[f]	0.45 ± 0.03[k]	≥90[g]
Intramolecular G4	0.55 ± 0.17[a]	1.0 ± 0.1 nt/s[h]	0.15 ± 0.01[i]	73[j]

[a] From Fig. 3*C*.
[b] Calculated by multiplying the single cycle unwinding rate constant from Fig. 2*C* by the kinetic step size of 1 bp/step previously determined for Pif1 (44) ($k_u \times 1$ bp/step).
[c] Calculated based on the sequence with an adjustment for the salt concentration (69).
[d] Measured at 20 °C (44).
[e] Data from Ref. 18.
[f] Calculated from the single cycle unwinding rate constant from Fig. 2*C* assuming that all nucleotides from the first tetrad guanine to the last tetrad guanine must be separated by Pif1 ($k_u \times 22$ nt).
[g] Data from Ref. 62.
[h] Calculated from the single cycle unwinding rate constant from Fig. 9*D* assuming that all nucleotides from the first guanine of the first G4 column to the last guanine of the third column must be separated by Pif1 ($k_u \times 12$ nt).
[i] From Fig. 9*D*.
[j] Data from Ref. 70.
[k] From Fig. 2*C*.

difficulty in unfolding of a parallel, intramolecular G4 is simply due to the stability of the structure.

Pif1 binds to ss/G4DNA junctions much more tightly than to ssDNA or ss/dsDNA junctions (Fig. 3). Hence, slower unfolding does not mean that the G4DNA substrates are not preferred in cells because the tight binding interactions could direct Pif1 to these sites. Because of the multiple factors that can be used to compare substrate quality, the preferred substrate depends on the parameter that is chosen. Although a short duplex is unwound at a faster rate than the parallel G4DNA (Fig. 2), it may not always be the best substrate. Because of the high affinity of Pif1 for G4DNA, tetramolecular G4DNA is unwound more completely than dsDNA at low Pif1 concentrations (18). Thus, depending on the conditions such as the enzyme concentration, the type of G4DNA, the length of the duplex, and the length of the ssDNA tail, the preferred substrate can vary. The most important factors are likely whether the substrate is melted in a time frame sufficient for biological relevance and the quantity of product formed. Ultimately comparing the activity of Pif1 for unwinding dsDNA and G4DNA will require a detailed understanding of the chemical and kinetic mechanisms of G4DNA unfolding.

The slowest unfolding rates were observed with the intramolecular G4DNA (Table 2). It is possible that tight binding of Pif1 to the quadruplex requires disruption of these interactions for unfolding to occur, resulting in a slower unfolding rate. We suggest that the c-MYC substrate is unfolded with a different rate-limiting step than that of the tetramolecular quadruplex or duplex DNA. The inefficiency of the unfolding reaction in terms of the ATP usage and the slower ATP hydrolysis rate indicates that additional kinetic and/or chemical events must occur to unfold the parallel quadruplex.

Pif1 has clear biological relevance functioning on sequences that fold into quadruplex structures. Pif1 was shown to localize to G4DNA-forming sequences in cells (16). In addition to extensive work from Zakian and co-workers (17, 18), human minisatellite CEB1, which contains a quadruplex-forming sequence, was introduced into yeast, leading to gross chromosomal rearrangements (63). When the G4DNA was mutated to reduce quadruplex formation, the gross chromosomal rearrangement rate was reduced by 30-fold. In *pif1*Δ cells, CEB1-induced gross chromosomal rearrangement was increased by 100-fold. The CEB1 sequence was recently shown to form a "snapback" parallel structure when examined by NMR (64). In light of our results comparing single cycle *versus* multiple cycle unfolding of a parallel G4DNA, it is possible that multiple Pif1 molecules act at the site of parallel quadruplexes in cells. This might be accomplished through cooperative interactions between Pif1 molecules such as dimerization (65). If relatively long regions of ssDNA occur adjacent to the quadruplex, then multiple Pif1 molecules might bind and increase activity through "functional cooperativity" (39). Alternatively, other proteins may also aid in G4DNA unfolding. The mitochondrial single-stranded DNA-binding protein Rim1 enhances dsDNA unwinding by Pif1 (41). It is possible that Rim1 or replication protein A, the nuclear single-stranded DNA-binding protein, affects G4DNA unfolding. Human replication protein A has been shown to unfold some G4 structures by itself (66), suggesting that Pif1 could work in cooperation with a single-stranded DNA-binding protein to unfold G4DNA.

In a previous report (19) studying unfolding of quadruplexes from the human telomeric sequence, unfolded product did not accumulate due to rapid refolding; instead, Pif1 patrolled the substrate and repetitively unfolded the G4DNA. By patrolling, Pif1 could make ssDNA available when needed for replication or repair. It is possible that Pif1 does patrol the parallel G4DNA substrates used here without completely unfolding the quadruplex structure. A partially unfolded G4DNA would likely not be trapped as dsDNA so it would appear as if Pif1 did not unfold it. The results from the reporter assay (Fig. 9) provide the outcome for fully unfolded parallel G4DNA. Additionally, we have found that Pif1 can accelerate annealing of complementary DNA strands (56). Therefore, it is possible that Pif1 can anneal duplex DNA in its wake as it unfolds G4DNA. Such activity would prevent refolding of G4DNA. It is possible that by converting the intramolecular G4DNA into dsDNA through unfolding/annealing Pif1 might prevent the G4 structure from refolding and leave behind a stable duplex structure.

Acknowledgments—We thank Sanjay Bharti and Robert Brosh for technical assistance.

REFERENCES

1. Byrd, A. K., and Raney, K. D. (2012) Superfamily 2 helicases. *Front. Biosci.* **17,** 2070–2088
2. Raney, K. D., Byrd, A. K., and Aarattuthodiyil, S. (2013) Structure and Mechanisms of SF1 DNA Helicases. *Adv. Exp. Med. Biol.* **767,** 17–46
3. Gilhooly, N. S., Gwynn, E. J., and Dillingham, M. S. (2013) Superfamily 1 helicases. *Front. Biosci.* **5,** 206–216
4. Brosh, R. M., Jr. (2013) DNA helicases involved in DNA repair and their roles in cancer. *Nat. Rev. Cancer* **13,** 542–558
5. Bochman, M. L., Paeschke, K., and Zakian, V. A. (2012) DNA secondary structures: stability and function of G-quadruplex structures. *Nat. Rev. Genet.* **13,** 770–780
6. Belotserkovskii, B. P., De Silva, E., Tornaletti, S., Wang, G., Vasquez, K. M., and Hanawalt, P. C. (2007) A triplex-forming sequence from the human c-MYC promoter interferes with DNA transcription. *J. Biol. Chem.* **282,** 32433–32441
7. Wang, G., Christensen, L. A., and Vasquez, K. M. (2006) Z-DNA-forming sequences generate large-scale deletions in mammalian cells. *Proc. Natl. Acad. Sci. U.S.A.* **103,** 2677–2682
8. Inagaki, H., Ohye, T., Kogo, H., Kato, T., Bolor, H., Taniguchi, M., Shaikh, T. H., Emanuel, B. S., and Kurahashi, H. (2009) Chromosomal instability mediated by non-B DNA: cruciform conformation and not DNA sequence is responsible for recurrent translocation in humans. *Genome Res.* **19,** 191–198
9. Bhattacharyya, B., and Keck, J. L. (2014) Grip it and rip it: structural mechanisms of DNA helicase substrate binding and unwinding. *Protein Sci.* **23,** 1498–1507
10. Zhao, J., Bacolla, A., Wang, G., and Vasquez, K. M. (2010) Non-B DNA structure-induced genetic instability and evolution. *Cell. Mol. Life Sci.* **67,** 43–62
11. Murat, P., and Balasubramanian, S. (2014) Existence and consequences of G-quadruplex structures in DNA. *Curr. Opin. Genet. Dev.* **25,** 22–29
12. Schaffitzel, C., Berger, I., Postberg, J., Hanes, J., Lipps, H. J., and Plückthun, A. (2001) *In vitro* generated antibodies specific for telomeric guanine-quadruplex DNA react with *Stylonychia lemnae* macronuclei. *Proc. Natl. Acad. Sci. U.S.A.* **98,** 8572–8577
13. Biffi, G., Tannahill, D., McCafferty, J., and Balasubramanian, S. (2013) Quantitative visualization of DNA G-quadruplex structures in human cells. *Nat. Chem.* **5,** 182–186

14. Henderson, A., Wu, Y., Huang, Y. C., Chavez, E. A., Platt, J., Johnson, F. B., Brosh, R. M., Jr., Sen, D., and Lansdorp, P. M. (2014) Detection of G-quadruplex DNA in mammalian cells. *Nucleic Acids Res.* **42,** 860–869
15. Müller, S., Kumari, S., Rodriguez, R., and Balasubramanian, S. (2010) Small-molecule-mediated G-quadruplex isolation from human cells. *Nat. Chem.* **2,** 1095–1098
16. Paeschke, K., Capra, J. A., and Zakian, V. A. (2011) DNA replication through G-quadruplex motifs is promoted by the *Saccharomyces cerevisiae* Pif1 DNA helicase. *Cell* **145,** 678–691
17. Ribeyre, C., Lopes, J., Boulé, J. B., Piazza, A., Guédin, A., Zakian, V. A., Mergny, J. L., and Nicolas, A. (2009) The yeast Pif1 helicase prevents genomic instability caused by G-quadruplex-forming CEB1 sequences *in vivo*. *PLoS Genet.* **5,** e1000475
18. Paeschke, K., Bochman, M. L., Garcia, P. D., Cejka, P., Friedman, K. L., Kowalczykowski, S. C., and Zakian, V. A. (2013) Pif1 family helicases suppress genome instability at G-quadruplex motifs. *Nature* **497,** 458–462
19. Zhou, R., Zhang, J., Bochman, M. L., Zakian, V. A., and Ha, T. (2014) Periodic DNA patrolling underlies diverse functions of Pif1 on R-loops and G-rich DNA. *Elife* **3,** e02190
20. Gray, L. T., Vallur, A. C., Eddy, J., and Maizels, N. (2014) G quadruplexes are genomewide targets of transcriptional helicases XPB and XPD. *Nat. Chem. Biol.* **10,** 313–318
21. Sarkies, P., Reams, C., Simpson, L. J., and Sale, J. E. (2010) Epigenetic instability due to defective replication of structured DNA. *Mol. Cell* **40,** 703–713
22. Huppert, J. L., and Balasubramanian, S. (2007) G-quadruplexes in promoters throughout the human genome. *Nucleic Acids Res.* **35,** 406–413
23. Todd, A. K., Johnston, M., and Neidle, S. (2005) Highly prevalent putative quadruplex sequence motifs in human DNA. *Nucleic Acids Res.* **33,** 2901–2907
24. Capra, J. A., Paeschke, K., Singh, M., and Zakian, V. A. (2010) G-quadruplex DNA sequences are evolutionarily conserved and associated with distinct genomic features in *Saccharomyces cerevisiae*. *PLoS Comput. Biol.* **6,** e1000861
25. Xiao, S., Zhang, J. Y., Zheng, K. W., Hao, Y. H., and Tan, Z. (2013) Bioinformatic analysis reveals an evolutional selection for DNA:RNA hybrid G-quadruplex structures as putative transcription regulatory elements in warm-blooded animals. *Nucleic Acids Res.* **41,** 10379–10390
26. Sen, D., and Gilbert, W. (1988) Formation of parallel four-stranded complexes by guanine-rich motifs in DNA and its implications for meiosis. *Nature* **334,** 364–366
27. Wu, Y., Shin-ya, K., and Brosh, R. M., Jr. (2008) FANCJ helicase defective in Fanconia anemia and breast cancer unwinds G-quadruplex DNA to defend genomic stability. *Mol. Cell. Biol.* **28,** 4116–4128
28. London, T. B., Barber, L. J., Mosedale, G., Kelly, G. P., Balasubramanian, S., Hickson, I. D., Boulton, S. J., and Hiom, K. (2008) FANCJ is a structure-specific DNA helicase associated with the maintenance of genomic G/C tracts. *J. Biol. Chem.* **283,** 36132–36139
29. Lopes, J., Piazza, A., Bermejo, R., Kriegsman, B., Colosio, A., Teulade-Fichou, M. P., Foiani, M., and Nicolas, A. (2011) G-quadruplex-induced instability during leading-strand replication. *EMBO J.* **30,** 4033–4046
30. Mohaghegh, P., Karow, J. K., Brosh, R. M., Jr., Bohr, V. A., and Hickson, I. D. (2001) The Bloom's and Werner's syndrome proteins are DNA structure-specific helicases. *Nucleic Acids Res.* **29,** 2843–2849
31. Bharti, S. K., Sommers, J. A., George, F., Kuper, J., Hamon, F., Shin-ya, K., Teulade-Fichou, M. P., Kisker, C., and Brosh, R. M., Jr. (2013) Specialization among iron-sulfur cluster helicases to resolve G-quadruplex DNA structures that threaten genomic stability. *J. Biol. Chem.* **288,** 28217–28229
32. Creacy, S. D., Routh, E. D., Iwamoto, F., Nagamine, Y., Akman, S. A., and Vaughn, J. P. (2008) G4 resolvase 1 binds both DNA and RNA tetramolecular quadruplex with high affinity and is the major source of tetramolecular quadruplex G4-DNA and G4-RNA resolving activity in HeLa cell lysates. *J. Biol. Chem.* **283,** 34626–34634
33. Giri, B., Smaldino, P. J., Thys, R. G., Creacy, S. D., Routh, E. D., Hantgan, R. R., Lattmann, S., Nagamine, Y., Akman, S. A., and Vaughn, J. P. (2011) G4 resolvase 1 tightly binds and unwinds unimolecular G4-DNA. *Nucleic Acids Res.* **39,** 7161–7178
34. Meier, M., Patel, T. R., Booy, E. P., Marushchak, O., Okun, N., Deo, S., Howard, R., McEleney, K., Harding, S. E., Stetefeld, J., and McKenna, S. A. (2013) Binding of G-quadruplexes to the N-terminal recognition domain of the RNA helicase associated with AU-rich element (RHAU). *J. Biol. Chem.* **288,** 35014–35027
35. Ambrus, A., Chen, D., Dai, J., Jones, R. A., and Yang, D. (2005) Solution structure of the biologically relevant G-quadruplex element in the human c-MYC promoter. Implications for G-quadruplex stabilization. *Biochemistry* **44,** 2048–2058
36. Qin, Y., and Hurley, L. H. (2008) Structures, folding patterns, and functions of intramolecular DNA G-quadruplexes found in eukaryotic promoter regions. *Biochimie* **90,** 1149–1171
37. Morris, P. D., Tackett, A. J., Babb, K., Nanduri, B., Chick, C., Scott, J., and Raney, K. D. (2001) Evidence for a functional monomeric form of the bacteriophage T4 Dda helicase. Dda does not form stable oligomeric structures. *J. Biol. Chem.* **276,** 19691–19698
38. Carroll, S. S., Benseler, F., and Olsen, D. B. (1996) Preparation and use of synthetic oligoribonucleotides as tools for study of viral polymerases. *Methods Enzymol.* **275,** 365–382
39. Byrd, A. K., and Raney, K. D. (2004) Protein displacement by an assembly of helicase molecules aligned along single-stranded DNA. *Nat. Struct. Mol. Biol.* **11,** 531–538
40. Bachrati, C. Z., and Hickson, I. D. (2006) Analysis of the DNA unwinding activity of RecQ family helicases. *Methods Enzymol.* **409,** 86–100
41. Ramanagoudr-Bhojappa, R., Blair, L. P., Tackett, A. J., and Raney, K. D. (2013) Physical and functional interaction between yeast Pif1 helicase and Rim1 single-stranded DNA binding protein. *Nucleic Acids Res.* **41,** 1029–1046
42. Ali, J. A., and Lohman, T. M. (1997) Kinetic measurement of the step size of DNA unwinding by *Escherichia coli* UvrD helicase. *Science* **275,** 377–380
43. Ali, J. A., Maluf, N. K., and Lohman, T. M. (1999) An oligomeric form of *E. coli* UvrD is required for optimal helicase activity. *J. Mol. Biol.* **293,** 815–834
44. Ramanagoudr-Bhojappa, R., Chib, S., Byrd, A. K., Aarattuthodiyil, S., Pandey, M., Patel, S. S., and Raney, K. D. (2013) Yeast Pif1 helicase exhibits a one-base-pair stepping mechanism for unwinding duplex DNA. *J. Biol. Chem.* **288,** 16185–16195
45. Eoff, R. L., and Raney, K. D. (2006) Intermediates revealed in the kinetic mechanism for DNA unwinding by a monomeric helicase. *Nat. Struct. Mol. Biol.* **13,** 242–249
46. Lahaye, A., Leterme, S., and Foury, F. (1993) PIF1 DNA helicase from *Saccharomyces cerevisiae*. Biochemical characterization of the enzyme. *J. Biol. Chem.* **268,** 26155–26161
47. Boulé, J. B., and Zakian, V. A. (2007) The yeast Pif1p DNA helicase preferentially unwinds RNA DNA substrates. *Nucleic Acids Res.* **35,** 5809–5818
48. Galletto, R., and Tomko, E. J. (2013) Translocation of *Saccharomyces cerevisiae* Pif1 helicase monomers on single-stranded DNA. *Nucleic Acids Res.* **41,** 4613–4627
49. Wang, Y., and Patel, D. J. (1993) Solution structure of the human telomeric repeat d[AG3(T2AG3)3] G-tetraplex. *Structure* **1,** 263–282
50. Parkinson, G. N., Lee, M. P., and Neidle, S. (2002) Crystal structure of parallel quadruplexes from human telomeric DNA. *Nature* **417,** 876–880
51. Ambrus, A., Chen, D., Dai, J., Bialis, T., Jones, R. A., and Yang, D. (2006) Human telomeric sequence forms a hybrid-type intramolecular G-quadruplex structure with mixed parallel/antiparallel strands in potassium solution. *Nucleic Acids Res.* **34,** 2723–2735
52. Halder, K., and Chowdhury, S. (2005) Kinetic resolution of bimolecular hybridization versus intramolecular folding in nucleic acids by surface plasmon resonance: application to G-quadruplex/duplex competition in human c-myc promoter. *Nucleic Acids Res.* **33,** 4466–4474
53. Eddy, S., Ketkar, A., Zafar, M. K., Maddukuri, L., Choi, J. Y., and Eoff, R. L. (2014) Human Rev1 polymerase disrupts G-quadruplex DNA. *Nucleic Acids Res.* **42,** 3272–3285
54. Zhang, A. Y., and Balasubramanian, S. (2012) The kinetics and folding pathways of intramolecular G-quadruplex nucleic acids. *J Am. Chem. Soc.* **134,** 19297–19308

55. Gray, R. D., Trent, J. O., and Chaires, J. B. (2014) Folding and unfolding pathways of the human telomeric G-quadruplex. *J. Mol. Biol.* **426,** 1629–1650
56. Ramanagoudr-Bhojappa, R., Byrd, A. K., Dahl, C., and Raney, K. D. (2014) Yeast Pif1 accelerates annealing of complementary DNA strands. *Biochemistry* **53,** 7659–7669
57. Ying, L., Green, J. J., Li, H., Klenerman, D., and Balasubramanian, S. (2003) Studies on the structure and dynamics of the human telomeric G quadruplex by single-molecule fluorescence resonance energy transfer. *Proc. Natl. Acad. Sci. U.S.A.* **100,** 14629–14634
58. Singleton, M. R., Dillingham, M. S., Gaudier, M., Kowalczykowski, S. C., and Wigley, D. B. (2004) Crystal structure of RecBCD enzyme reveals a machine for processing DNA breaks. *Nature* **432,** 187–193
59. Toseland, C. P., Martinez-Senac, M. M., Slatter, A. F., and Webb, M. R. (2009) The ATPase cycle of PcrA helicase and its coupling to translocation on DNA. *J. Mol. Biol.* **392,** 1020–1032
60. Serebrov, V., and Pyle, A. M. (2004) Periodic cycles of RNA unwinding and pausing by hepatitis C virus NS3 helicase. *Nature* **430,** 476–480
61. Long, X., Parks, J. W., Bagshaw, C. R., and Stone, M. D. (2013) Mechanical unfolding of human telomere G-quadruplex DNA probed by integrated fluorescence and magnetic tweezers spectroscopy. *Nucleic Acids Res.* **41,** 2746–2755
62. Sen, D., and Gilbert, W. (1990) A sodium-potassium switch in the formation of four-stranded G4-DNA. *Nature* **344,** 410–414
63. Piazza, A., Serero, A., Boulé, J. B., Legoix-Né, P., Lopes, J., and Nicolas, A. (2012) Stimulation of gross chromosomal rearrangements by the human CEB1 and CEB25 minisatellites in *Saccharomyces cerevisiae* depends on G-quadruplexes or Cdc13. *PLoS Genet.* **8,** e1003033
64. Adrian, M., Ang, D. J., Lech, C. J., Heddi, B., Nicolas, A., and Phan, A. T. (2014) Structure and conformational dynamics of a stacked dimeric G-quadruplex formed by the human CEB1 minisatellite. *J. Am. Chem. Soc.* **136,** 6297–6305
65. Barranco-Medina, S., and Galletto, R. (2010) DNA binding induces dimerization of *Saccharomyces cerevisiae* Pif1. *Biochemistry* **49,** 8445–8454
66. Ray, S., Qureshi, M. H., Malcolm, D. W., Budhathoki, J. B., Celik, U., and Balci, H. (2013) RPA-mediated unfolding of systematically varying G-quadruplex structures. *Biophys. J.* **104,** 2235–2245
67. Narayana, N., and Weiss, M. A. (2009) Crystallographic analysis of a sex-specific enhancer element: sequence-dependent DNA structure, hydration, and dynamics. *J. Mol. Biol.* **385,** 469–490
68. Gavathiotis, E., and Searle, M. S. (2003) Structure of the parallel-stranded DNA quadruplex d(TTAGGGT)4 containing the human telomeric repeat: evidence for A-tetrad formation from NMR and molecular dynamics simulations. *Org. Biomol. Chem.* **1,** 1650–1656
69. Kibbe, W. A. (2007) OligoCalc: an online oligonucleotide properties calculator. *Nucleic Acids Res.* **35,** W43–W46
70. Hatzakis, E., Okamoto, K., and Yang, D. (2010) Thermodynamic stability and folding kinetics of the major G-quadruplex and its loop isomers formed in the nuclease hypersensitive element in the human c-Myc promoter: effect of loops and flanking segments on the stability of parallel-stranded intramolecular G-quadruplexes. *Biochemistry* **49,** 9152–9160